Prominent Inclusion Effect of Dimethyl-β-cyclodextrin on Photoisomerization of the Thromboxane Synthetase Inhibitor (*E*)-4-(1-Imidazoylmethyl)cinnamic Acid

FUMITOSHI HIRAYAMA*, TADANOBU UTSUKI*, KANETO UEKAMA*x, MASAKI YAMASAKI‡, AND KAZUAKI HARATA§

Received April 30, 1991, from the *Faculty of Pharmaceutical Sciences, Kumamoto University, 5-1, Oe-honmachi, Kumamoto 862, Japan, the ‡Department of Bioengineering, Yatsushiro National College of Technology, 2627 Hirayama-shinmachi, Yatsushiro, Kumamoto 866, Japan, and the §Research Institute for Polymer and Textiles, 1-1-4 Higashi, Tsukuba, Ibaraki 305, Japan. Accepted for publication September 26, 1991.

Abstract □ The direct photoisomerization of (*E*)-4-(1-imidazoylmethyl)-cinnamic acid (IMC), a thromboxane synthetase inhibitor, to its (*Z*)-isomer at pH 2.0 was decelerated by β-cyclodextrin (β-CyD) and heptakis(2,6-di-*O*-methyl)-β-cyclodextrin (DM-β-CyD). The photostationary composition [(*Z*)-isomer:IMC ratio] was shifted in favor of IMC. These effects were much greater with DM-β-CyD than with the parent β-CyD. The quantum yield of the photoisomerization was significantly decreased by complex formation with β-CyDs, whereas the extinction coefficient of the guest was only slightly decreased. This situation was in sharp contrast to those observed in less polar solvents and suggests that the suppressing mechanism with β-CyD is different from that with less polar solvent systems. Spectroscopic studies (ultraviolet, circular dichroism, and nuclear magnetic resonance) indicated that IMC is tightly included in an axial mode in the cavity of DM-β-CyD and that the rotation of the photoreactive site is sterically hindered. The results suggest that the suppressing effect of β-CyDs on the photoisomerization of IMC results mainly from a steric origin.

Cyclodextrins (CyDs) are cyclic oligosaccharides consisting of more than six glucose units linked by α-1,4-glycosidic bonds. They can encapsulate appropriately sized guest molecules within their hydrophobic cavities.[1] The photochemical reactivities of the entrapped guest molecules can be significantly modified by such reactions. Fries, Smiles, and Claisen rearrangements,[2-4] Norrish type I and II reactions,[5] nucleophilic substitutions,[6] *trans–cis* isomerizations,[7] dimerizations,[8] and oxidations.[9] Recently, chemically modified CyD derivatives have received considerable attention with regard to the construction of artificial enzymes,[10] analytical reagents,[11] and drug delivery carriers.[12] From the viewpoints of reaction control and drug stabilization, CyD derivatives with enhanced inclusion ability are preferable to the parent CyDs. However, the use of modified CyDs in the photochemistry field has been relatively limited. We reported[13,14] that chlorpromazine and clomipramine, tricyclic antidepressants, were selectively dechlorinated when photoirradiated with β-CyDs, and this effect was much greater with heptakis(2,6-di-*O*-methyl)-β-CyD (DM-β-CyD) than with the parent β-CyD. The photodecarboxylation of benoxaprofen, an anti-inflammatory drug, was also decelerated by DM-β-CyD.[15] The amplified effect offered by DM-β-CyD in modifying the rates and pathways of photoreactions is due to the superior inclusion ability of the host with the extended hydrophobic cavity.[16] We have investigated the direct $E \rightarrow Z$ photoisomerization of (*E*)-4-(1-imidazoylmethyl)cinnamic acid (IMC; Scheme I), a thromboxane synthetase inhibitor,[17] that was embedded in the DM-β-CyD cavity. The decelerating mechanism of DM-β-CyD is discussed on the basis of the inclusion structure of the complex.

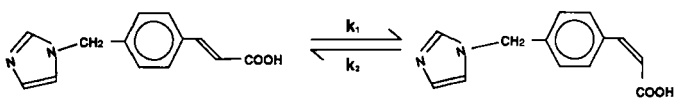

IMC (*Z*)-isomer

Scheme I—Photoisomerization of IMC.

Experimental Section

Materials—IMC and the (*Z*)-isomer were donated by Kissei Pharmaceutical Company (Matsumoto, Japan). β-CyD (Nihon Shokuhin Kako Company, Tokyo, Japan) was recrystallized from water. DM-β-CyD (Toshin Chemical Company, Tokyo, Japan) was used after recrystallization from methanol (3×) and water (1×) and was confirmed to be a single component by high-performance liquid chromatography (HPLC) and fast-atom-bombardment mass spectrometry (Jeol JMS-DX303HF, Tokyo, Japan). All other chemicals and solvents were of analytical reagent grade, and deionized double-distilled water was used.

Spectroscopy—Circular dichroism (CD) and UV spectra were recorded with a Jasco J-50A recording polarimeter and a Hitachi U-3200 spectrometer, respectively. All measurements were carried out in pH 2.0 phosphate buffer [ionic strength (μ), 0.2] at 25 °C. Proton (^{1}H) and carbon-13 (^{13}C) nuclear magnetic resonance (NMR) spectra were recorded at 25 °C on a Jeol JNM FX-270 spectrometer operating at 270.17 and 67.94 MHz, respectively, with sweep widths of 2700 and 15 000 Hz, respectively. The concentrations of the host and guest were 1.0×10^{-2} M in D_3PO_4 solution (pH 1.5). ^{1}H and ^{13}C NMR chemical shifts are given in parts per million (ppm) downfield from that of sodium 2,2-dimethyl-2-silapentane-5-sulfonate, as an external reference, with accuracies of ±0.0011 and ±0.014 ppm, respectively. Two-dimensional (2D) NMR spectra [correlation spectroscopy (COSY) and 2D rotating frame nuclear Overhauser effect spectroscopy (ROESY)] were recorded on Jeol JNM-EX 400 or GX-400 spectrometers operating at 399.65 MHz (^{1}H NMR) and 100.40 MHz (^{13}C NMR). Representative parameters used to obtain the 2D NMR spectra were as follows: ^{1}H–^{1}H COSY: sweep width, 4000 Hz; scan, 64 every evolution period (t_1) with a pulse delay of 1 s; data matrix, zero-filled to 512 × 1k (1k is 1 kilobyte of memory); and spectrum processing, sine bell window function with apodization in both dimensions; ^{1}H–^{13}C COSY: sweep widths, 25 000 Hz (^{13}C) and 4000 Hz (^{1}H); delay times, 3.6 and 1.8 ms; scan, 750 every t_1 with a pulse delay of 1 s; data matrix, 2k × 128 in frequency dimensions (ω_1 and ω_2); final matrix, 2k × 512; phase-sensitive ROESY: sweep width, 3501.4 Hz; carrier frequency, 5.6 ppm; spin-lock field, 4 kHz; mixing time, 250 ms; scan, 64 every t_1 with a pulse delay of 2.4 s; data matrix, 2 × 256 × 512. The NMR signals of IMC were assigned with the aid of 2D ^{1}H–^{1}H and ^{1}H–^{13}C COSY experiments, and those of DM-β-CyD were assigned according to the report of Inoue and co-workers.[18]

Photolysis—IMC solution (1.0×10^{-4} M in pH 2.0 phosphate buffer, 20 mL) was placed in a 50-mL heat-resistant (Pyrex) beaker (45 mm i.d. × 70 mm; thickness, 1.4 mm) with a Pyrex stopper and was irradiated at 25 °C, with a merry-go-round-type apparatus. The light source was a UV-B lamp (Toshiba FL20SE-30, Tokyo) that emits at 290–320 nm, with a maximum at 305 nm. The distance from the

0022-3549/92/0800-0817$02.50/0

sample solution to the lamp was ~350 mm, and the energy intensity was ~0.1 mW/cm^2 at 305 nm. At appropriate intervals, an aliquot (1.0 mL) was sampled and analyzed for IMC and the (*Z*)-isomer by HPLC under the following conditions: column, octadecyl silica gel reversed-phase column (LiChrosorb RP-18, 10 μm, 4 mm i.d. × 250 mm); mobile phase, 0.3% ammonium acetate:methanol (7:2, v/v); flow rate, 1.0 mL/min; detection, UV at 272 nm; internal standard, benzoic acid. Aerobic and anaerobic conditions were set up by bubbling the solutions with oxygen and nitrogen, respectively, for 30 min.

Quantum Yield—Light intensities were measured with a ferrioxalate actinometer[19] equipped with a double quartz cell (path length of each cell, 1.0 cm; face, 2.5 × 1.0 cm); that is, IMC (1.0×10^{-4} M in pH 2.0 phosphate buffer) and potassium ferrioxalate (6.0×10^{-3} M in 0.05 M sulfuric acid) solutions were put in the front and rear cells, respectively. Side faces of the cell were covered with black paper to avoid entrance of incident light. The cell was positioned in a housing in front of the lamp and was irradiated through a Pyrex glass. At appropriate times [within 5% conversion of IMC to the (*Z*)-isomer], IMC and the (*Z*)-isomer were determined by HPLC, and the resulting ferrous ion was determined spectrophotometrically at 510 nm after complexation with 1,10-phenanthroline. A quantum yield of 1.24 was used for the formation of ferrous ion at 305 nm.[19] The quantum yield (0.69) was determined with (*E*)-cinnamic acid under the same conditions as a quantum standard and was in good agreement with the value (0.70) reported by Bolte et al.[20]

Results

Effects of DM-β-CyD on Photoisomerization of IMC—Figure 1 shows typical photoisomerization profiles of IMC in the absence and presence of DM-β-CyD in phosphate buffer (pH 2.0). The pH condition was chosen for the convenience of kinetic measurements, because isomerization at alkaline condition was very slow. The isomerization obeyed reversible first-order kinetics, and the mass balance of IMC and the (*Z*)-isomer was >98%, indicating no appreciable side reaction, such as dimerization, under the given experimental conditions. Table I summarizes the forward (k_1) and backward (k_2) rate constants and the photostationary compositions [K = (*Z*)-isomer:IMC]. The K values were in good agreement with the ratio k_1:k_2. The forward reaction was decelerated 2.0 and 1.6 times by the addition of DM-β-CyD and β-CyD, respectively, and the backward reaction was decelerated ~1.3 times. The photostationary composition (2.82–3.43) of the β-CyD systems was shifted in favor of IMC, compared with that (4.37) without β-CyDs. The isomerization of IMC was also retarded in less polar solvents, such as water–methanol, that mimic the apolar environment of the CyD cavity, although the photostationary composition in such solvents shifted in favor of the (*Z*)-isomer.

Quantum yields of the photoisomerization of the IMC (ϕ_E) and the (*Z*)-isomer (ϕ_Z) are summarized in Table II. The ϕ_Z values were calculated from eq 1[21]:

$$[(Z)\text{-isomer}]/[\text{IMC}] = (\phi_E \cdot \varepsilon_E)/(\phi_Z \cdot \varepsilon_Z) \qquad (1)$$

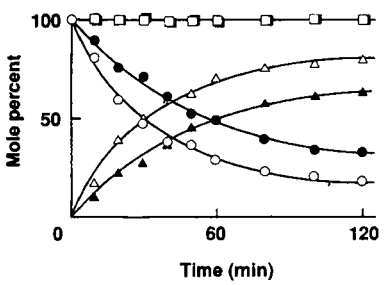

Figure 1—Photoisomerization profiles of IMC in the absence and presence of DM-β-CyD (5.0×10^{-3} M) in phosphate buffer (pH 2.0, μ = 0.2) at 25 °C. Key: (○) IMC without β-CyDs; (△) (*Z*)-isomer without β-CyDs; (□) IMC + (*Z*)-isomer without β-CyDs; (●) IMC with DM-β-CyD; (▲) (*Z*)-isomer with DM-β-CyD; (■) IMC + (*Z*)-isomer with DM-β-CyD.

Table I—Photoisomerization Rate Constants (k_1 and k_2) and Photostationary Compositions (K) of IMC in Various Systems[a]

System	$k_1 \times 10^2$, min	$k_2 \times 10^2$, min	K
IMC alone	2.63 ± 0.08	0.602 ± 0.018	4.4 ± 0.2
With β-CyD[b]	1.64 ± 0.07	0.478 ± 0.026	3.4 ± 0.1
With DM-β-CyD[b]	1.30 ± 0.08	0.496 ± 0.002	2.8 ± 0.1
In 50% methanol[c]	1.84 ± 0.08	0.380 ± 0.012	4.9 ± 0.2
In 50% dioxane[c]	1.19 ± 0.04	0.279 ± 0.002	4.3 ± 0.1

[a] Values are expressed as means ± standard deviations. [b] 5.0×10^{-3} M. [c] In phosphate buffer (pH 2.0; μ = 0.2) at 25 °C.

Table II—Photoisomerization Quantum Yields (ϕ)[a] and Extinction Coefficients (ε)[b] of IMC in Various Systems

System	ε_E	ε_Z	ϕ_E	ϕ_Z
IMC alone	8.71	2.34	0.26	0.22
With β-CyD[c]	7.84	2.34	0.18	0.17
With DM-β-CyD[c]	7.11	2.41	0.15	0.15
In 50% methanol[d]	7.60	1.40	0.26	0.29
In 50% dioxane[d]	7.52	2.04	0.25	0.22

[a] Concentration of IMC was 1.0×10^{-4} M; standard error in ϕ was within ±0.005. [b] At 305 nm ($\times 10^{-3}$). [c] 5.0×10^{-3} M. [d] In phosphate buffer (pH 2.0; μ = 0.2) at 25 °C.

In eq 1, [IMC] and [(*Z*)-isomer] are the molar concentrations of IMC and the (*Z*)-isomer, respectively, at the photostationary state, and ϵ_E and ϵ_Z are the extinction coefficients of IMC and the (*Z*)-isomer, respectively, at 305 nm. The quantum yields of the forward and backward reactions of IMC were lowered from 0.26 and 0.22 to 0.15 by the addition of DM-β-CyD; this reduction is greater than that caused by the parent β-CyD. β-CyDs lowered predominantly the quantum yields rather than the extinction coefficients. This situation was in contrast to those observed in less polar solvents [i.e., in methanol solution, the extinction coefficients were predominantly lowered, whereas the quantum yields were almost constant or slightly increased (0.26–0.29)]. These results suggest that the suppressing mechanism of β-CyDs is different from that of less polar solvents; that is, β-CyDs affect the photochemical (e.g., isomerization) or photophysical (e.g., nonradiative decay) process of IMC after the Frank–Condon excitation, whereas the light-absorbing efficiency, an initial photophysical step of reactions, is suppressed in less polar solvents.

Inclusion Complex Formation of IMC with DM-β-CyD—Spectroscopic studies (UV, CD, and NMR) of the formation of the IMC–β-CyD inclusion complex were conducted, because the change in reactivity of IMC seemed to be induced mainly by a steric effect of the CyDs rather than by a solvent effect. Figure 2 shows UV and CD spectra of IMC in the absence and presence of DM-β-CyD and β-CyD. The UV absorption spectrum of IMC was simply the superposition of the spectra of cinnamic acid and 1-methylimidazole and was little affected by the addition of β-CyDs. On the other hand, IMC showed a new induced CD band at ~270–280 nm due to the binding to β-CyDs, and the intensity was higher with DM-β-CyD than with β-CyD. Figure 3 shows the continuous variation plots[22] of the changes in ellipticity of IMC at 275 nm. Both β-CyD systems gave a peak at a 1:1 molar ratio of the guest and host, indicating a 1:1 stoichiometry of the complexes. Formation constants, K_c = [complex]/[guest] [host], of the 1:1 complexes were determined by analyzing the induced CD changes as a function of CyD concentration by means of the Scott method.[23] As shown in Table III, the inclusion ability of DM-β-CyD for both IMC and the (*Z*)-isomer was much greater than that of the parent β-CyD. Scheme II shows the proposed equilibria at the photostationary state, where K_{c1} and K_{c2} are formation constants for IMC and the (*Z*)-isomer complexes, respectively,

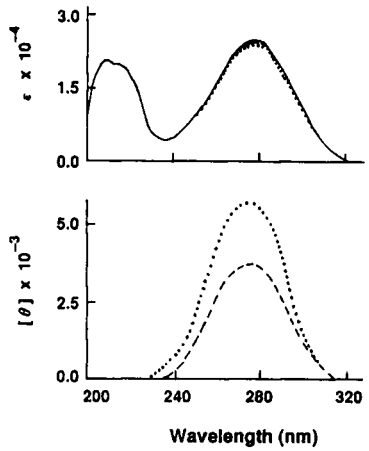

Figure 2—UV (**Top**) and CD (**Bottom**) spectra of IMC (5.0×10^{-5} M) in the absence and presence of β-CyDs (2.5×10^{-3} M) in phosphate buffer (pH 2.0, $\mu = 0.2$) at 25 °C. Key: (——) without β-CyDs; (– – –) with β-CyD; (· · · ·) with DM-β-CyD.

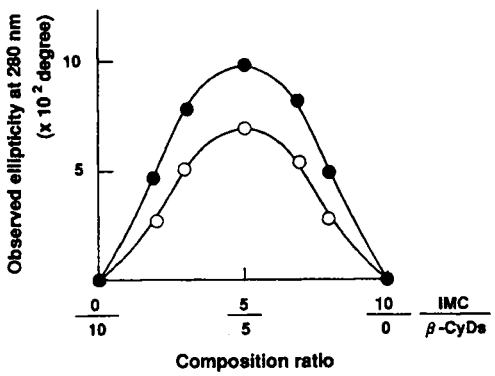

Figure 3—Continuous variation plots for IMC–β-CyD systems in phosphate buffer (pH 2.0, $\mu = 0.2$) at 25 °C. Key: (○) with β-CyD; (●) with DM-β-CyD. Total concentration of IMC and β-CyDs was 5.0×10^{-4} M.

Table III—Formation Constants (K_c)[a] of β-CyD Complexes with IMC and (*Z*)-Isomer[b]

Host	K_{C1}, M^{-1}[c]	K_{C2}, M^{-1}[d]
β-CyD	510 ± 10	390 ± 10
DM-β-CyD	1390 ± 30	740 ± 20

[a] Values expressed as mean ± standard error. [b] In phosphate buffer (pH 2.0; $\mu = 0.2$) at 25 °C. [c] Complex with IMC. [d] Complex with (*Z*)-isomer.

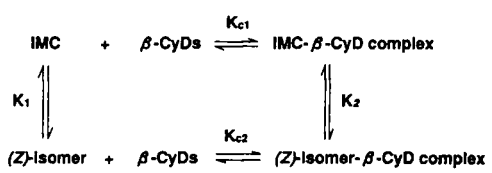

Scheme II—Equilibria of IMC–β-CyD complexes at photostationary state.

and K_1 and K_2 are photostationary compositions (Table I) of IMC and the complex, respectively. These constants must bear the following relation in the closed equilibrium: $K_{c1}K_2 = K_{c2}K_1$. In fact, the observed values fulfilled this relation, within experimental error: $K_{c1}K_2/K_{c2}K_1 = 1.0$–$1.2$.

The electronic transition of the included guest with a transition dipole moment parallel to the z axis of the CyD cavity (Figure 4) gives a positive CD, and that with a transition dipole moment perpendicular to the z axis gives a negative CD.[24] To gain insight into the inclusion structure, therefore, the theoretical rotational strengths (R_{oa}) of IMC in the β-CyD complexes were calculated with eqs 2 and 3, which were developed by Tinoco,[25] and compared with the experimental values (the details of the calculation method and symbols are found in the work of Harata[24,26]):

$$R_{oa} = \pi \nu_a \mu_{oa}^2 \sum_i \frac{\nu_i^2(\alpha_{33} - \alpha_{11})_i(\mathrm{GF})_i}{c(\nu_i^2 - \nu_a^2)} \qquad (2)$$

$$(\mathrm{GF})_i = \frac{1}{r_i^2}[(e_a \cdot e_i) - 3(e_a \cdot e_{oi})(e_i \cdot e_{oi})](e_a \times e_i) \cdot e_{oi} \qquad (3)$$

The dependence of the calculated value of R_{oa} on the distance (d) between the center of the electric dipole moment (μ_{oa}) of IMC and that of the DM-β-CyD cavity (Figure 4) are shown in Figure 5 (left panel). R_{oa} was calculated by placing the μ_{oa} vector along the z axis and moving the center of the vector from −5 to 5 Å in increments of 0.5 Å. The center of the DM-β-CyD cavity was fixed at the center of gravity of the plane consisting of the seven glycosidic oxygens (Figure 4). The calculated R_{oa} value depends on the angle (ψ) between the μ_{oa} vector (located at the gravity) and the z axis (Figure 5, right panel) as the μ_{oa} vector is rotated around the y axis from 0 to 90° in increments of 10°. A maximum CD band with positive sign can be observed when the center of the μ_{oa} vector is located ~2 Å below the plane of the glycosidic oxygens (Figure 5). The positive CD intensity of IMC will decrease with increasing inclination of the μ_{oa} vector from the z axis, and the positive sign changes to a negative sign when the ψ value is beyond ~50°. The experimental rotational strengths (R) of the DM-β-CyD and β-CyD complexes were determined to be 6.27×10^{40} and 4.94×10^{40} cgsu (cgs units), respectively, by analyzing the UV and CD spectral data (Figure 2) according to eq 4[27]:

$$R = 0.696 \times 10^{-42} \pi^{1/2} [\theta]_{max} \Delta / \lambda_{max} \qquad (4)$$

In eq 4, $[\theta]_{max}$ is the maximum value of the molar ellipticity, Δ is the half-band width at $1/e$ of maximum ellipticity, and λ_{max} is the wavelength at the absorption maximum. These results indicate that the center of the μ_{oa} vector of IMC should be located within the range ~−3.5–1 Å from the glycosidic plane of DM-β-CyD to give an R value of $>6.27 \times 10^{40}$ cgsu and that its direction should be slightly inclined from the z

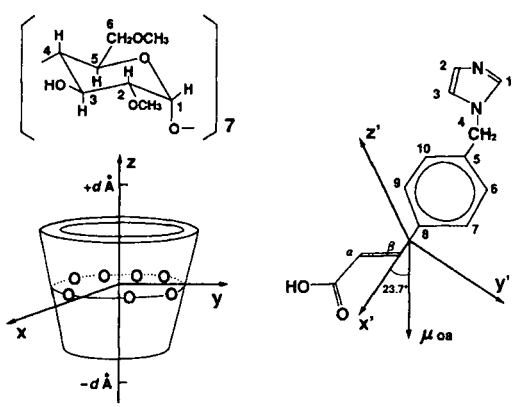

Figure 4—Coordinate systems and carbon numberings for IMC (**Right**) and glucose unit of DM-β-CyD (**Left**).

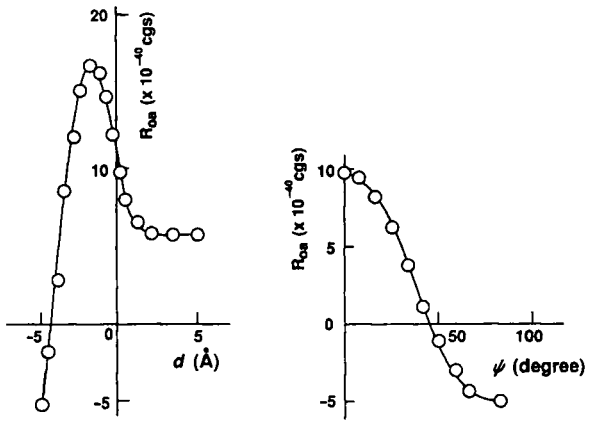

Figure 5—Dependence of calculated R_{oa} values on distance (*d*; **Left**) and angle (ψ; **Right**).

axis. Compared with the DM-β-CyD complex, the μ_{oa} center in the β-CyD complex may be moved 0.5 Å further to the narrow side of the cavity, consisting of the methylated primary hydroxyl groups. Molecular orbital calculations on cinnamic acid[28] suggest that the UV absorption band of IMC around 270 nm can be assigned to an intramolecular charge-transfer band and that its transition moment is directed to 23.7° with respect to the x′ axis of IMC (Figure 4). Therefore, we assume that the IMC molecule is included in an axial mode in β-CyDs [i.e., the x′ axis of IMC is parallel to the z axis of the cavity (Figure 6), and IMC is included more deeply in the DM-β-CyD cavity than in the β-CyD cavity].

The inclusion structure of the IMC–DM-β-CyD complex was further confirmed by NMR spectroscopic studies. Table IV and Figure 7 summarize the ^{13}C NMR chemical shifts and shift changes of the guest and host molecules for the IMC–DM-β-CyD system. The ^{13}C NMR signals (C1 and C2) of the imidazole moiety were largely shifted downfield (1.07 and 0.52 ppm, respectively), whereas the signals due to C3–C10 carbons were shifted upfield. The acrylic acid moiety showed an alternating change of sign (−1.79, 0.65, −1.38, and 0.058 ppm for the COOH, Cα, Cβ, and C8 carbons, respectively). Inoue et al.[29] showed that, theoretically, the carbons included in the hydrophobic cavity are largely shielded compared with the deshielded carbons located around the wider side of the CyD cavity consisting of secondary hydroxyl groups. Therefore, the results (Figure 7) suggest that the benzene moiety of IMC is situated in the hydrophobic center of the DM-β-CyD cavity and that the imidazole moiety is located around the wider side of the cavity or oriented outside of the cavity. The alternative carbon-13 displacement of the acrylic acid moiety may be due to the enhanced inductive effect of the carboxylic acid in the hydrophobic CyD cavity.[30] The IMC-induced ^{13}C NMR shift changes of DM-β-CyD were relatively large for the C1, C3, C5, and C6 carbons of the host. The large shift changes of the C1 and C6 carbons may be due to conformational

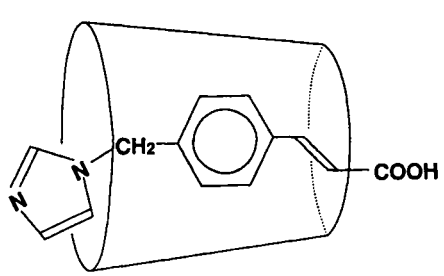

Figure 6—Proposed inclusion structure of IMC–DM-β-CyD complex in solution.

Table IV—^{13}C NMR Chemical Shift Changes of IMC and DM-β-CyD for IMC–DM-β-CyD System in pH 1.5 Phosphate Buffer

Carbon	Chemical Shift of IMC, ppm		
	δ_0[a]	δ_{CyD}[b]	$\Delta\delta$[c]
C1	136.09	137.16	1.07
C2	120.10	120.62	0.52
C3	121.98	121.68	−0.30
C4	52.31	52.09	−0.22
C5	134.81	134.44	−0.37
C6, C10	129.08	128.95	−0.13
C7, C9	128.97	128.38	−0.59
C8	134.81	134.87	0.06
Cβ	145.45	144.07	−1.38
Cα	118.40	119.05	0.65
COOH	170.79	169.01	−1.79
	Chemical Shift of DM-β-CyD, ppm		
	δ_0[d]	δ_{IMC}[e]	$\Delta\delta_{CyD}$[f]
C1	99.25	99.49	0.25
C2	81.39	81.35	−0.04
C3	72.15	72.38	0.23
C4	81.25	81.67	0.14
C5	70.02	70.26	0.25
C6	70.65	70.41	−0.24
C2–OCH_3	59.31	59.45	0.14
C6–OCH_3	58.40	58.43	0.03

[a] Chemical shift of IMC alone. [b] Chemical shift of IMC with DM-β-CyD. [c] $\delta_{CyD} - \delta_0$. [d] Chemical shift of DM-β-CyD alone. [e] Chemical shift of DM-β-CyD with IMC. [f] $\delta_{IMC} - \delta_0$.

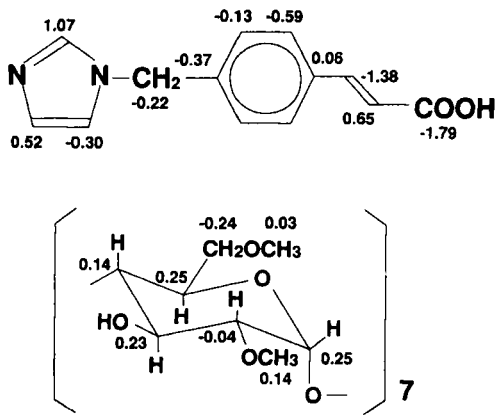

Figure 7—^{13}C NMR chemical shift displacements (ppm) of IMC (1.0×10^{-2} M) and DM-β-CyD (1.0×10^{-2} M) due to inclusion complexation in phosphate buffer (pH 1.5). Positive values indicate downfield shifts, and negative values indicate upfield shifts.

changes around the glycosidic bond and the C5–C6 bond, respectively, through the inclusion of IMC, because of the high flexibility of these bonds. The large shifts of the C3 and C5 carbons may support the formation of an inclusion complex with IMC, because these carbons are located inside the cavity. In the ^1H NMR spectra, the H3 proton of DM-β-CyD showed a marked upfield shift (0.249 ppm), whereas the shifts of the H1, H2, and H4 protons, which are located outside the cavity, were small (<0.02 ppm). The H5 signal of DM-β-CyD could not be measured accurately with the 270-MHz spectrometer because of overlapping with the H6 signals. The parent β-CyD gave similar ^{13}C and ^1H NMR displacements, although the magnitude of the changes was less than that for DM-β-CyD.

ROESY is particularly useful for detecting nuclei that are in close proximity and provides information on the orientation of IMC with respect to the CyD cavity.[31–33] Figure 8 shows complete and partial contour plots of the ROESY spectrum of the IMC–DM-β-CyD system. The cross peaks connecting the intermolecular protons are as follows: (1) the C4–H resonance of IMC to the C2–OCH_3 resonance of DM-β-CyD and (2) the Cα–H resonance of IMC to the C6–OCH_3 resonance of DM-β-CyD. The essentially identical cross peaks were observed also in the nuclear Overhauser effect spectroscopy (NOESY) spectrum of the DM-β-CyD complex. These cross peaks are due only to the nuclear Overhauser effect, because they arise between two protons belonging to two different molecules; they suggest the close contact (<4–5 Å) of the interacting protons. Figure 6 shows the inclusion structure of the IMC–DM-β-CyD complex in solution, which we propose on the basis of the spectroscopic results. The IMC molecule is assumed to be included in the DM-β-CyD cavity with the carboxylic acid moiety located around the narrow side of the cavity and with the imidazole moiety located around the wide side of the cavity. The β-CyD complex may have a similar inclusion structure, although the inclusion of IMC is shallow.

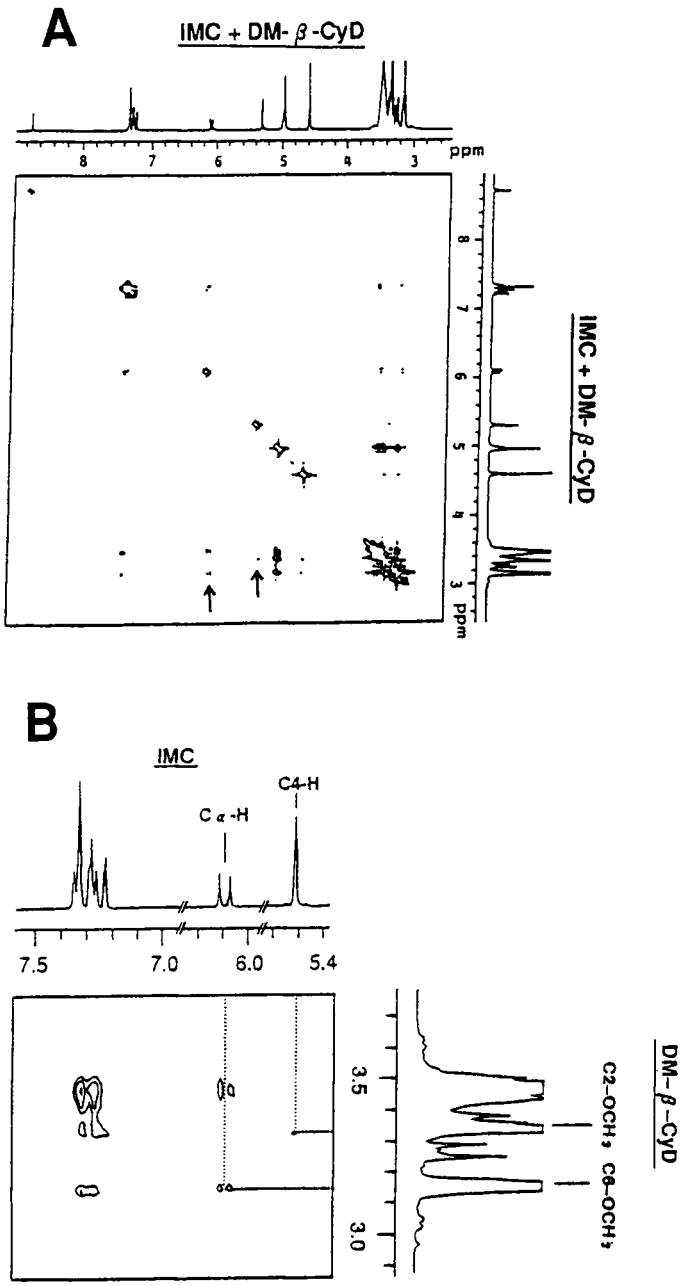

Figure 8—Complete (**A**) and partial (**B**) contour plots of ROESY spectrum of IMC (2.0×10^{-2} M)–DM-β-CyD (2.0×10^{-2} M) system in phosphate buffer (pH 1.5). The cross peaks between IMC and DM-β-CyD resonances are shown by the arrows and dotted lines.

Discussion

β-CyDs suppressed the photoisomerization of IMC. The effect was greater with DM-β-CyD than with the parent β-CyD. The quantum yield of the photoreaction was significantly decreased by inclusion complexation with β-CyDs, whereas the light-absorbing efficiency of IMC was little affected, in sharp contrast to results obtained in less polar solvents. These results suggest that β-CyD affects the photophysical or photochemical decay process after the excitation, whereas the light-absorbing efficiency (an initial photophysical process) of the guest is suppressed in less polar solvents. Furthermore, these results suggest that steric factors play a dominant role in the photochemistry of the complexes, because the absorptivity of the guest at the wavelength of the light source in the free state was nearly identical to that in the complexed state.

The direct $E \rightarrow Z$ photoisomerization of cinnamic acid shows a marked multiplicity dependence on *para* substituents of the benzene ring[34] (i.e., the reaction proceeds via a singlet state in the case of unsubstituted, *p*-methyl-, *p*-methoxy-, and *p*-chlorocinnamic acids). It proceeds via a triplet state in the case of the *p*-nitro, *p*-acetyl and *p*-cyano derivatives. The direct photoisomerization of IMC may proceed via a singlet state, because IMC is a *p*-methylcinnamic acid derivative and no oxygen quenching was observed (i.e., ϕ_E and K in the absence of CyDs were 0.26 and 4.35, respectively, under anaerobic conditions and 0.26 and 4.37, respectively, under aerobic conditions; these values in the presence of DM-β-CyD were 0.15 and 2.82, respectively, under anaerobic conditions and 0.15 and 2.78, respectively, under aerobic conditions). Furthermore, no degradation of the imidazole moiety, a substrate of singlet oxygen, of IMC was observed; therefore, singlet oxygen was not produced.[35]

The sum of ϕ_E and ϕ_Z for the photoisomerization of (*E*)-cinnamic acid in aqueous solution (pH 2.0) is 1 ($\phi_E = 0.7$ and $\phi_Z = 0.3$),[20] indicating isomerization without competing nonradiative decay. On the other hand, the sum of ϕ_E and ϕ_Z for IMC was ~0.5 and decreased to 0.3 after complexation with DM-β-CyD. Because IMC was nonfluorescent at room temperature even in the complexed state, in the lowest singlet state of (*E*)-cinnamic acid,[36] nonradiative decay may compete efficiently with the isomerization of IMC. After light absorption, the IMC molecule is excited to a higher excited singlet state, maintaining the planar configuration of the double bond of the styryl moiety, and decays to the ground state through the lowest excited singlet state, which has a twisted configuration.[21] The excitation ratios of IMC in the free and complexed states can be almost the same owing to similar extinction coefficients. Therefore, β-CyDs may inhibit the decay pathways from the higher to the lowest excited singlet states (planar to twisted configurations) or from the lowest excited singlet state to the ground state (twisted to planar configurations), because the rotational freedom of the reactive site is at least partly lost in the β-CyD cavity, as expected from the structure of the inclusion complex. This loss of rotational freedom would favor the nonradiative decay of IMC in the complex. Such steric hindrance by DM-β-CyD was reflected in the larger decrease of ϕ_E (0.26 to 0.15) relative to that of ϕ_Z (0.22 to 0.15), because the isomerization of (*E*)-cinnamic acids

to (*Z*)-forms has a higher rotational barrier compared with the reverse reaction.[21]

Ramamurthy and co-workers[37] reported that the $E \rightarrow Z$ photoisomerization of cinnamic acid esters was little affected by β-CyD. However, the photoisomerization of IMC was significantly decelerated by DM-β-CyD, with the enhanced inclusion ability and the photostationary composition also shifted in favor of IMC. Therefore, DM-β-CyD is much more useful than the parent β-CyD in controlling photoreactions, particularly for stabilization of photolabile drugs of certain sizes.

References and Notes

1. Bender, M. L.; Komiyama, M. *Cyclodextrin Chemistry*; Springer-Verlag: Berlin, 1978.
2. Veglia, A. V.; Sanchez, A. M.; de Rossi, R. H. *J. Org. Chem.* **1990**, *55*, 4083–4086.
3. Wubbels, G. G.; Sevetson, B. R.; Kaganove, S. N. *Tetrahedron Lett.* **1986**, *27*, 3103–3106.
4. Syamala, M. S.; Ramamurthy, V. *Tetrahedron* **1988**, *23*, 7223–7233.
5. Rao, B. N.; Syamala, M. S.; Turro, N. L.; Ramamurthy, V. *J. Org. Chem.* **1987**, *52*, 5517–5521.
6. Liu, J. H.; Weiss, R. G. *Isr. J. Chem.* **1985**, *25*, 228–232.
7. Bortolus, P.; Monti, S. *J. Phys. Chem.* **1987**, *91*, 5046–5050.
8. Rideout, D. C.; Breslow, R. *J. Am. Chem. Soc.* **1980**, *102*, 7816–7817.
9. Yamada, K.; Shigehiro, K.; Tomizawa, T.; Iida, H. *Bull. Chem. Soc. Jpn.* **1978**, *51*, 3302–3306.
10. Breslow, R. *Science* **1982**, *218*, 532–537.
11. Armstrong, D. W.; Ward, T. J.; Armstrong, R. D.; Beesley, T. E. *Science* **1986**, *232*, 1132–1135.
12. Uekama, K.; Otagiri, M. *CRC Crit. Rev. Ther. Drug Carrier Syst.* **1987**, *3*, 1–40.
13. Uekama, K.; Irie, T.; Hirayama, F. *Chem. Lett.* **1978**, 1109–1112.
14. Hoshino, T.; Irie, T.; Hirayama, F.; Uekama, K.; Yamasaki, M. *Yakugaku Zasshi* (in Japanese) **1989**, *109*, 107–112.
15. Hoshino, T.; Ishida, K.; Irie, T.; Hirayama, F.; Uekama, K. *J. Incl. Phenom.* **1988**, *6*, 415–423.
16. Harata, K.; Hirayama, F.; Uekama, K.; Tsoucaris, G. *Chem. Lett.* **1988**, 1585–1588.
17. Iizuka, K.; Akahane, K.; Momose, D.; Makazawa, M.; Tanouchi, T.; Kawamura, M.; Ohyama, I.; Kajiwara, I.; Iguchi, Y.; Okada, T.; Taniguchi, K.; Miyamoto, T.; Hayashi, M. *J. Med. Chem.* **1981**, *24*, 1139–1148.
18. Yamamoto, Y.; Onda, M.; Takahashi, Y.; Inoue, Y.; Chujo, R. *Carbohydr. Res.* **1987**, *170*, 229–234.
19. Parker, C. A. *Proc. Royal Soc. London* **1953**, *A220*, 104–117.
20. Bolte, M.; Lorain, C.; Lemaire, J. *C. R. Acad. Sci. Paris* **1981**, *293*, 817–820.
21. Lewis, F. D.; Oxman, J. D.; Gibson, L. L.; Hampsch, H. L.; Quillen, S. L. *J. Am. Chem. Soc.* **1986**, *108*, 3005–3015.
22. Job, P. *Ann. Chem.* **1928**, *9*, 113–203.
23. Scott, R. L. *Rec. Trav. Chim.* **1956**, *75*, 787–789.
24. Harata, K. *Bull. Chem. Soc. Jpn.* **1975**, *48*, 375–378.
25. Tinoco, I., Jr. *Adv. Chem. Phys.* **1962**, *4*, 113–160.
26. Harata, K. *Bioorg. Chem.* **1981**, *10*, 255–265.
27. Djerassi, C. *Optical Rotatory Dispersion*; McGraw-Hill: New York, 1960.
28. Nakamura, K.; Kikuchi, S. *Bull. Chem. Soc. Jpn.* **1967**, *40*, 1027–1030.
29. Inoue, Y.; Hoshi, H.; Sakurai, M.; Chujo, R. *J. Am. Chem. Soc.* **1985**, *107*, 2319–2323.
30. Straub, T. S.; Bender, M. L. *J. Am. Chem. Soc.* **1972**, *94*, 8875–8881.
31. Bothner-By, A. A.; Stephens, R. L.; Lee, J.; Warren, C. D.; Jeanloz, R. W. *J. Am. Chem. Soc.* **1984**, *106*, 811–813.
32. Bergeron, R.; Rowan R., III *Bioorg. Chem.* **1976**, *5*, 425–436.
33. Inoue, Y.; Kanda, Y.; Yamamoto, Y.; Chujo, R.; Kobayashi, S. *Carbohydr. Res.* **1989**, *194*, C8–C13.
34. Ishigami, T.; Nakazato, K.; Uehara, M.; Endo, T. *Tetrahedron Lett.* **1979**, *10*, 863–866.
35. Koizumi, M.; Kato, S.; Mataga, N.; Matsuura, T.; Usui, Y. *Photosensitized Reactions*; Kagakudojin Publishing: Kyoto, Japan, 1978; pp 210–241.
36. Nakamura, K.; Kikuchi, S. *Bull. Chem. Soc. Jpn.* **1968**, *41*, 1977–1982.
37. Syamala, M. S.; Devanathan, S.; Ramamurthy, V. *J. Photochem.* **1986**, *34*, 219–229.

Acknowledgments

We are grateful to Dr. T. Imanari (Jeol Ltd., Tokyo, Japan) for measurements of the 2D NMR spectra.